Multiscale simulation of flow-induced texture formation in thermotropic liquid crystals

D. Grecov* and A.D. Rey**

Department of Chemical Engineering, McGill University, 3610, University Street, Montreal, Quebec, Canada
* dana.grecov@mcgill.ca, ** alejandro.rey@mcgill.ca

ABSTRACT

This paper presents theory and simulation of flow-induced structures, useful to the creation of synthetic material structures and to the biomimetics of natural fibers. We present a multiscale theory and simulation of hydrodynamic texture formation to provide fundamental principles for control and optimization of structures in liquid crystal polymers. In thermotropic flow-aligning nematic polymers it found that as the shear-rate increases, the pathway between an oriented non-planar state and an oriented planar state is through texture formation and coarsening, temperature and shear rate being efficient fields to control the grain size of the texture. High temperatures and shear rates lead to defect free monodomains. The texture transition cascade: *unoriented monodomain* $\Rightarrow$ *defect lattice* $\Rightarrow$ *defect gas* $\Rightarrow$ *oriented monodomain* is remarkably consistent with the experimentally observed textural transitions of sheared lyotropic nematic polymers.

Keywords: shear flow, liquid crystal polymers, textural transformations, inversion wall, defects

1. INTRODUCTION

The orientational order of liquid crystals offers a unique pathway to create new nano and microstructures with unique optical, electromagnetic, and mechanical properties. In addition, liquid crystal biomimetics offers the appropriate tools to understand how Nature produces high performance fibers, such as spider silk. This paper presents theory and simulation of flow-induced structures, useful to the creation of synthetic material structures and to the biomimetics of natural fibers.

Nematic liquid crystals (NLCs) are textured, anisotropic, viscoelastic materials. Their mechanical behavior is greatly influenced by the presence of textures, or spatial distribution of topological defects. The theoretical and computational framework for the widely reported flow-induced texture and pattern formation phenomena in liquid crystal materials, has been investigated in several studies [1].

The role of shear on texture formation and texture coarsening is greatly affected on the flow properties of NLCs [1], the molecular weight (i.e. low-molar mass or polymeric), the temperature and the class of NLC (i.e. lyotropic or thermotropic [2]). Figure 1 shows an schematic of the molecular geometry, positional disorder, and uniaxial orientational order of rigid rod nematic polymers (NPs). The partial orientational order of the molecular unit axis **u** is along the average orientation given by the director **n** (**n**·**n**=1). The shear flow behaviour and rheology of nematic liquid crystals (NLCs) depend on the sign and magnitude of the reactive parameter λ, which is the ratio of the flow aligning effect of the deformation rate and the tumbling (rotational) effect of the vorticity [2]. For rods-like NLCs it is known that $\lambda>0$ [1]. When $\lambda > 1$ the material flow aligns close to the velocity direction since the rotational effect of vorticity is overcome by deformation. When $0 < \lambda <1$ the director does not align close to the velocity direction because the rotational effect of vorticity dominates over the aligning effect of deformation. Materials with $\lambda >1$ display the flow-aligning mode. No systematic data that shows that thermotropic liquid crystals, such as Vectra [3], are non-aligning materials, has been presented. At present there appears to be consensus that thermotropic nematic polymers are flow-aligning [4].

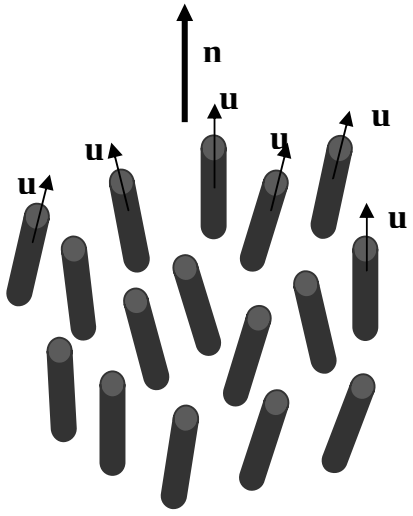

Figure 1: Schematic of the molecular geometry, positional disorder, and uniaxial orientational order of rigid rod liquid crystal polymers. The partial orientational order of the

molecular unit axis **u** is along the average orientation given by the director **n** (**n**·**n**=1)

Textures are spatial distributions of defects. Inversion walls are 2D non-singular defects, in which spatially localized twist rotations occur. Once nucleated, inversion walls can shrink, pinch, or annihilate with other walls or other defects [5]. Since sheared flow-aligning nematic polymer orient very close to the velocity direction, inversion wall formation is expected if the initial orientation is orthogonal to the imposed flow. In this paper we use shear-induced generation of twist inversion walls as a model for texture generation.

The aim of this paper is to elucidate the flow principle mechanisms that control textural transformation in sheared, flow-aligning, rigid-rod, nematic polymers, as function of shear rate and temperature.

2. THEORY AND GOVERNING EQUATIONS

We present the Landau-de Gennes theory for nematic liquid crystals, and the parametric equations used to describe liquid crystalline polymers texture formation. The theory is well suited to simulate texture formation since defects are non-singular solutions to the governing equations. In this paper we study a rectilinear simple start-up shear flow with Cartesian coordinates, as shown in figure 2. The lower plate is fixed and the upper plate starts moving at t=0 with a known constant velocity V; the plate separation is H. The z axis is coaxial with the vorticity axis and the shear plane is span by the x-y axes.

The dynamics of the tensor order parameter is given by the following sum of flow **F**, short range $\mathbf{H}^{sr}$, and long range $\mathbf{H}^{lr}$ contributions [6]:

$$\frac{\partial \mathbf{Q}}{\partial t} + (\mathbf{v}\cdot\nabla)\mathbf{Q} - \mathbf{W}\cdot\mathbf{Q} + \mathbf{Q}\cdot\mathbf{W} = \mathbf{F}(\mathbf{Q},\nabla\mathbf{v}) + \mathbf{H} \qquad (1)$$

$$\mathbf{H} = \mathbf{H}^{sr}\left(\mathbf{Q},\bar{D}_r(\mathbf{Q})\right) + \mathbf{H}^{lr}(\nabla\mathbf{Q})$$

(i) flow contribution **F**:

$$\mathbf{F}(\mathbf{Q},\nabla\mathbf{v}) = \tfrac{2}{3}\beta\mathbf{A} + \beta\left[\mathbf{A}\cdot\mathbf{Q} + \mathbf{Q}\cdot\mathbf{A} - \tfrac{2}{3}(\mathbf{A}:\mathbf{Q})\mathbf{I}\right] - \tfrac{1}{2}\beta[(\mathbf{A}:\mathbf{Q})\mathbf{Q} + \mathbf{A}\cdot\mathbf{Q}\cdot\mathbf{Q} + \mathbf{Q}\cdot\mathbf{A}\cdot\mathbf{Q} + \mathbf{Q}\cdot\mathbf{Q}\cdot\mathbf{A} - \{(\mathbf{Q}\cdot\mathbf{Q}):\mathbf{A}\}\mathbf{I}] \qquad (2)$$

(ii) short-range elastic contribution $\mathbf{H}^{sr}$:

$$\mathbf{H}^{sr}\left(\mathbf{Q},\bar{D}_r(\mathbf{Q})\right) = -6\bar{D}_r[(1-\tfrac{1}{3}U)\mathbf{Q} - U\mathbf{Q}\cdot\mathbf{Q} + U\{(\mathbf{Q}:\mathbf{Q})\mathbf{Q} + \tfrac{1}{3}(\mathbf{Q}:\mathbf{Q})\mathbf{I}\}] \qquad (3)$$

(iii) long-range elastic contribution $\mathbf{H}^{lr}$:

$$\mathbf{H}^{lr}(\mathbf{Q}) = 6\bar{D}_r[\frac{L_1}{2ckT}\nabla^2\mathbf{Q} + \frac{1}{2}\frac{L_2}{c\kappa T}[\nabla(\nabla\cdot\mathbf{Q}) + \{\nabla(\nabla\cdot\mathbf{Q})\}^T - \tfrac{2}{3}\mathrm{tr}\{\nabla(\nabla\cdot\mathbf{Q})\}\mathbf{I}]] \qquad (4)$$

$$\bar{D}_r = \frac{Dr}{\left(1-\frac{3}{2}\mathbf{Q}:\mathbf{Q}\right)} \qquad (5)$$

Here **A**, L_i (i=1,2), U and β are the rate of deformation tensor , the Landau elastic coefficients, the nematic potential and the molecular shape parameter, respectively. $\bar{D}_r$ is the microstructure dependent rotational diffusivity. The dimensionless numbers Er (Ericksen number) and energy ratio R [6]:

$$Er = \frac{\dot{\gamma}H^2ckT^*}{2L_1D_r} \qquad R = \frac{3H^2ckT^*}{L_1} \qquad (6,7)$$

give the ratio of viscous flow effects to long-range order elasticity, and short-range order elasticity to long-range order elasticity, respectively (H is the distance between the two plates (see figure 2)),V is the constant velocity of the top plate, $\dot{\gamma}$ is the shear rate, T^* is the isotropic-nematic transition temperature), c is the concentration of molecules per unit volume and k the Boltzmann constant. The Deborah number De, or ratio between flow effect and short range energy effect is given by:

$$De = \frac{Er}{R} = \frac{\dot{\gamma}}{6D_r} \qquad (8)$$

and its magnitude controls the amplitude of effects associated with the scalar order parameters.

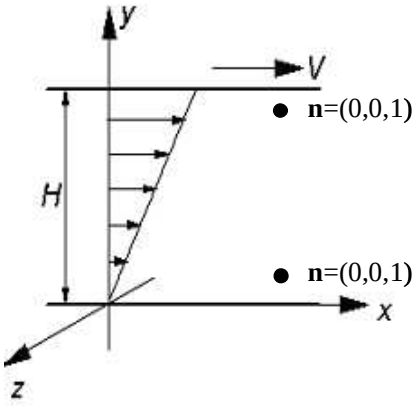

Figure 2: Definition of the flow geometry and coordinates system for simple shear flow. The lower plate is at rest and the upper plate moves in the x- direction with a constant velocity V. H is the gap separation.

The model equations (1) are a set of five coupled non-linear parabolic partial differential equations. The equations are solved using Galerkin Finite Elements for spatial discretization and a fourth order Runge-Kutta time adaptive method. Convergence and mesh-independence were established in all cases using standard methods. Spatial discretization was judiciously selected taking into account the length scale of our model. The selected adaptive time integration scheme is able to efficiently take

into account the stiffness that rises due to the disparity between time scales and length scales.

3. NUMERICAL RESULTS

In this work fixed boundary conditions are used, such that the director **n** is anchored along the vorticity direction (see figure 2). The initial state is assumed to be uniaxial and at equilibrium. The orientation of the director at t=0 is assumed to be parallel to the vorticity axis, with thermal fluctuations introduced by infinitesimal Gaussian noise. In the present work the parametric values are set at: β =1 and β =1.2 (flow aligning system). The selected ranges for the dimensionless parameters are: $R = 10^6$, $0<De<6$.

Previous work [7] has shown that as the Ericksen number increases, the Landau-deGennes theory predicts the existence of six stable steady state modes, as follows:

(1) Homogeneous mode (H): the director is aligned everywhere along the vorticity axis (n_z=1).

(2) Symmetric mode (S): the director reorients uniformly towards the shear plane, creating a symmetric twist angle profile. Since the reorientation has a unique sense (say clockwise) no twist wall appear at the center region.

(3) Asymmetric mode (A): the re-orientation direction in the top half-layer is opposite to the bottom half-layer. The resulting director field exhibits a twist wall at the center of the gap, and two boundary layers at the bounding surfaces.

(4) Defect lattice mode (DL): The number of re-orientation reversal increases with increasing shear rate, and the director filed display a finite number of twist inversion walls separated by a nearly constant distance. The mode is spatially periodic and the wave-length is the wall-wall distance. Since the mode is periodic it is denoted defect lattice.

a)

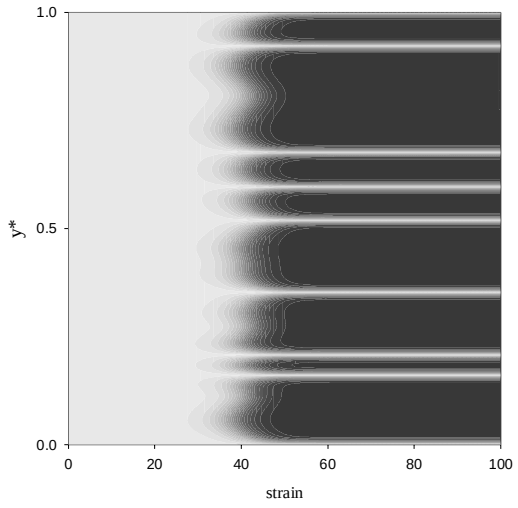

b)

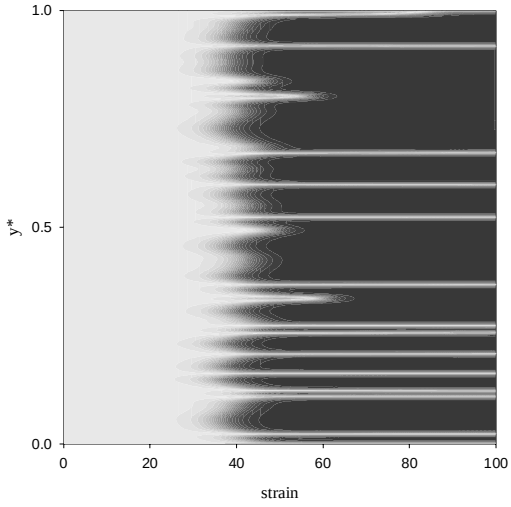

c)

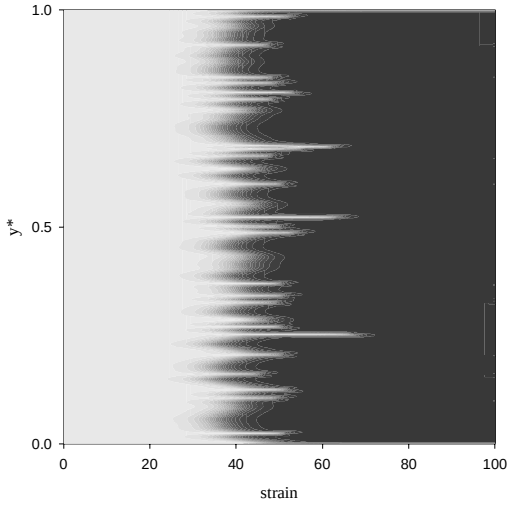

Figure 3: Gray-scale plot of the evolution in time of the out-of plane component n_z. White: n_z=1 (out of plane orientation), black: n_z=0 (in plane orientation), β =1, $R=10^6$, U=4.5: a) defect lattice mode, De=0.5; b) defect gas mode, De=1.9; c) Planar mode, De=4.6.

In this mode no coarsening processes (i.e., annihilation) occur. If annihilation takes place periodicity is destroyed.

(5) Defect gas mode (DG): in this mode annihilation processes set in and walls nucleate and react with other walls, with the bounding surfaces, and/or they pinch. Since coarsening is a random process it destroys periodicity and the mode is referred as a defect gas mode. The twist wall distance is a random variable.

(6) Planar mode (P): At the highest shear rates, annihilation by pinching overcomes nucleation, and no twist walls

remain at steady state. The resulting mode is planar and defect free.

Figure 3 shows computed gray scale visualizations of director component n_z ($0 \leq y^* \leq 1$) as a function of strain, corresponding to the three modes :a) defect lattice mode DL (De=0.5, $R=10^6$); b) defect gas mode DG (De=1.9, $R=10^6$) and c) planar P mode (De=4.2, $R=10^6$). Black represents in plane orientation ($n_z=0$) and light represents orientation along the vorticity ($n_z=1$) axis.

The steady state texture of a liquid crystal is given by the balance of nucleation and coarsening processes. Coarsening events limit the lifetime of an inversion wall, and a texture can be viewed as a balance between birth-death events. Coarsening processes of inversion walls under shear can involve: (a) pinching (see figure 3c) (b) wall-bounding surface reaction (see figure 3b) , and (c) wall-wall annihilation (see figure 3b) [7].

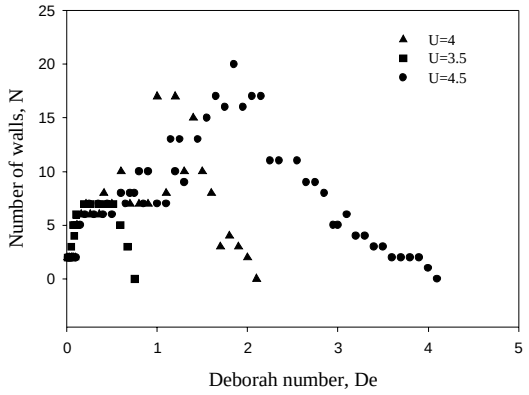

Figure 4**:** Twist walls number, N as a function of Deborah number, for different nematic potentials, U.

Figure 4 shows the number of inversion walls at steady state function of shear rate (De) for different temperatures (nematic potential, U) for $R=10^6$, $\beta=1.2$. At lower temperatures (higher U) the defect lattice mode and the defect gas mode persist for a larger range of Deborah numbers, De. The simulations show that control of texture formation is feasible by temperature and shear rate selection. To obtain a texture free sample (N=0), a sufficiently high shear rate (De) and temperature (U) are necessary.

4. CONCLUSIONS

Since the viscosities of polymeric nematics are invariably high, the Ericksen number in flow of these fluids is also almost always high i.e. Er $\sim 10^4$-10^6 or higher, so is very important to study the transitions that occur at this Ericksen numbers. The classical theories of nematodynamics applied to thermotropic rod-like shear-flow aligning nematic polymers predict that, as the shear-rate increases, the pathway between an oriented non-planar state and an oriented planar state is through texture formation and coarsening. The two shear-rate dependent dimensionless numbers that control the texture formation and coarsening process are Ericksen Er and Deborah De numbers. The emergence of texture is independent of the Deborah number, and occurs at $Er=10^4$. As the shear rate increases and $Er>10^4$ the first texture that arises is a lattice of inversion walls. Further increases of the shear rate, ignite the coarsening processes, and replace the defect lattice with a defect gas. Finally at higher shear rates, a monodomain state emerges, and the texture vanishes since coarsening overpowers defect nucleation. It is found that the texture transition cascade:

unoriented monodomain $\Rightarrow$ *defect lattice* $\Rightarrow$ *defect gas* $\Rightarrow$ *oriented monodomain* is remarkably consistent with the textural transition of sheared lyotropic tumbling nematic polymers [8].

Temperature and shear rate are efficient fields to control the grain size of the texture. High temperatures and shear rates lead to defect free monodomains. The flow simulations are shown to be in full agreement with experimental observations.

ACKNOWLEDGEMENTS

This work was supported primarily by the ERC Program of the National Science Foundation under Award Number EEC-9731680. DG acknowledges support from the Natural Science and Engineering Research Council of Canada.

REFERENCES

1. A.D Rey and M.M Denn, Annu.Rev.Fluid.Mech, 34 ,233, 2002.
2. R.G.Larson , *The structure and Rheology of Complex Fluids*, Oxford University Press, New York, 1999 .
3. F.Beekmans, A.D. Gotsis and B.Norder, J. Rheol., 40(5), 947, 1996.
4. V .M. Ugaz, W.R. Burghardt, W. Zhou and J. Kornfield , J. Rheol, 45, 1029, 2001.
5. A.D. Rey, Liquid Crystals, 7(3), 315-334 1990.
6. A. P. Singh and A. D. Rey, J. Non-Newtonian Fluid Mech., 94, 87,2000.
7. D.Grecov and A.D.Rey, Physical Review E, in press, 2003.
8. R. G. Larson, D.W. Mead, Liquid Crystals 15(2), 151 1993.